DOI: 10.1002/chem.200501066

Bis(trifluoromethyl)phosphinous Acid $(CF_3)_2$P-O-H: An Example of a Thermally Stable Phosphinous Acid—Synthesis, Gas-Phase Structure, and Rotational Isomers

Berthold Hoge,*[a] Placido Garcia,[b] Helge Willner,[b] and Heinz Oberhammer[c]

Dedicated to Professor Reint Eujen on the occasion of his 60th birthday

Abstract: The bis(trifluoromethyl)-phosphinous acid, $(CF_3)_2$P–O–H, is the only known example of a thermally stable phosphinous acid. Although this compound has been known since 1960, little is known about the chemistry of this extraordinary compound; this might be due to the tedious, and in some part risky, synthesis that was originally published. An improved, simple, and safe synthesis that is based on the treatment of the easily accessible $(CF_3)_2PNEt_2$, with at least three equivalents of *p*-toluene sulfonic acid, is presented. The reaction results in a complete conversion to the phosphinous acid, which is isolated in almost 90% yield. The compound exists in an equilibrium of two P–OH rotational isomers, a fact which is supported by quantum chemical calculations. The relative enthalpy difference of 6.4 kJ mol^{-1}, calculated at the B3PW91/6-311G(3d,p) level, is in excellent agreement with the experimental value of 5.9 kJ mol^{-1}, which was determined from the temperature dependence of the $\tilde{\nu}$(OH) bands of the two rotational isomers. The complete experimental vibrational spectra of both rotamers, their predicted vibrational spectra obtained by using quantum chemical calculations, and an attempt at photoinduced isomerization of matrix-isolated $(CF_3)_2$POH is presented. The experimental structure, obtained from an electron-diffraction study in the gas phase, is reproduced very well by ab initio and density functional theory (DFT) methods.

Keywords: density functional calculations · isomers · phosphinous acid · phosphorus · synthetic methods

Introduction

Secondary phosphane oxides (SPOs) exhibit phosphane oxide ($R_2P(O)H$)↔phosphinous acid (R_2P–O–H) tautomerism (R = alkyl, aryl). The equilibrium between the pentavalent phosphane oxide and the phosphinous acid with a trivalent phosphorus atom is almost completely shifted to the side of the phosphane oxide.[1]

As early as 1968, Chat and Heaton described the shift of the equilibrium to the side of the phosphinous acid form on coordination of the acid to transition-metal complexes [Eq. (1)].[2]

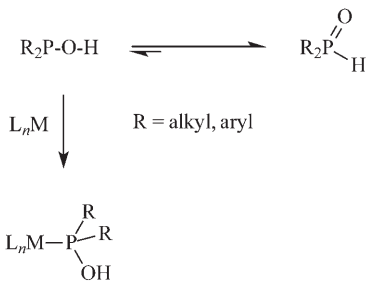

(1)

Due to their catalytic activity in homogeneous catalysis, transition-metal complexes of phosphinous acids are cur-

[a] Priv.-Doz. Dr. B. Hoge
Institut für Anorganische Chemie
Universität zu Köln
Greinstraße 6, 50939 Köln (Germany)
Fax: (+49) 221-470-5196
E-mail: b.hoge@uni-koeln.de

[b] Dr. P. Garcia, Prof. Dr. H. Willner
Fachbereich C, Anorganische Chemie
Bergische Universität Wuppertal
Gaußstraße 20, 42097 Wuppertal (Germany)

[c] Prof. Dr. H. Oberhammer
Institut für Physikalische und Theoretische Chemie
Universität Tübingen
72076 Tübingen (Germany)

rently of great interest, as was previously highlighted by Dubrovina and Börner.[3]

As established by theoretical and experimental investigations, the electron-withdrawing effect of the organic groups attached to the phosphorus atom strongly influences the equilibrium distribution between the phosphane oxide and phosphinous acid tautomers.[4,5] For the dimethyl derivative, only the oxide isomer could be observed so far. This observation is supported by density functional theory (DFT) calculations, which show that the corresponding phosphinous acid is 42 kJ mol^{-1} higher in energy. Depending on the electron-withdrawing effect of pentafluorophenyl and tetrafluoropyridinyl groups, the resulting phosphinous acids, $R_2P{-}O{-}H$ ($R = C_6F_5$, C_5NF_4), are stabilized with respect to the corresponding tautomeric oxide forms $R_2P(O)H$ by 1.7 and 10.5 kJ mol^{-1}, respectively. Based on this smaller energy difference, both derivatives exhibit a solvent-dependent equilibrium between their tautomeric forms.[5] The phosphinous acid $(CF_3)_2P{-}O{-}H$ is favored at the B3PW91/6-311G(3d,p) level of theory by a zero-point-corrected energy difference (ΔE_{ZP}) of about 14 kJ mol^{-1} relative to the phosphane oxide structure.

To date, the bis(trifluoromethyl)phosphinous acid, $(CF_3)_2P{-}O{-}H$, is the only known example of a thermally stable noncoordinated phosphinous acid. Although the phosphinous acid was already synthesized in 1960 by Burg and Griffiths,[6] little is known about the chemistry of this extraordinary compound.

Virlichie and Dagnac described the sensitivity of the phosphinous acid towards hydrolysis,[7] evolving HCF_3 as shown in Equation (2):

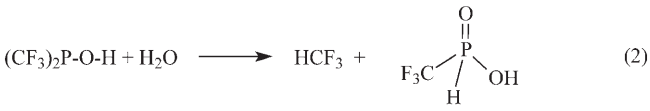

(2)

In addition, Burg mentioned the formation of a white solid on treatment of $(CF_3)_2POH$ with NEt_3, formulated as a phosphinite salt, $[NHEt_3]P(CF_3)_2O$.[6,8]

One reason why the chemistry of the only known phosphinous acid has not been investigated in detail might be its tedious, and in some part risky synthesis. The synthesis, published by Burg and Griffiths,[8] starts with $(CF_3)_2PI$, obtained by the autoclave reaction of CF_3I with elemental phosphorus. The anhydride of the phosphinous acid, the tetrakis(trifluoromethyl)diphosphoxane $(CF_3)_2P{-}O{-}P(CF_3)_2$, is obtained in 80% yield on treatment of $(CF_3)_2PI$ with silver carbonate. Before the product can be separated from the reaction mixture by means of fractional condensation, the unreacted $(CF_3)_2PI$ has to be converted to the removable $(CF_3)_2PCl$ by reaction with silver chloride.

The anhydride $(CF_3)_2P{-}O{-}P(CF_3)_2$ represents a unique compound showing no rearrangement to the diphosphane monoxide, and can be transformed into $(CF_3)_2PCl$ and $(CF_3)_2POH$ on reaction with gaseous HCl (86 h, 100 °C). The product $(CF_3)_2POH$ can be separated in a 90% yield by means of trap-to-trap condensation of the gaseous reaction mixture. For the reactions and purification, safety precautions are necessary, because $(CF_3)_2POH$, $(CF_3)_2POP(CF_3)_2$, and especially $(CF_3)_2PCl$ react violently with air.

Herein, we present for bis(trifluoromethyl)phosphinous acid, $(CF_3)_2POH$: 1) a safe, one step, and high-yield synthesis; 2) a complete spectroscopic characterization; 3) a structure determination obtained from an electron-diffraction study in the gas phase; and 4) a determination of the rotational equilibrium of its two isomers in the gas phase.

Results and Discussion

Trifluoromethylphosphorus derivatives are conveniently accessible by using the Ruppert procedure,[9] which was improved for the synthesis of $Et_2NP(CF_3)_2$ by Röschenthaler and co-workers.[10] The minor air sensitive, and therefore easily manageable, colorless liquid $(CF_3)_2PNEt_2$ was synthesized on a 100–200 g scale. In the presence of gaseous HBr, the amino phosphane was transformed into $(CF_3)_2PBr$.[11] The neat, volatile, colorless liquid, which explodes on contact with air, hydrolyzed in the presence of water yielding the target compound $(CF_3)_2POH$. To prevent the handling of $(CF_3)_2PBr$, the cleavage of the P–N bond of $(CF_3)_2PNEt_2$ and the following hydrolysis of the halogen derivative $(CF_3)_2PX$ can be performed in one step, by treating a solution of $(CF_3)_2PNEt_2$ in CH_2Cl_2 with aqueous HCl, as shown in Equation (3):

$$(CF_3)_2P{-}NEt_2 \xrightarrow[-[NEt_2H_2]Cl]{\text{concd HCl}} (CF_3)_2P{-}O{-}H \qquad (3)$$

However, the separation of $(CF_3)_2POH$ from the organic layer by means of fractional condensation was less successful, yielding $(CF_3)_2POH$ contaminated with variable amounts of water. At room temperature the mixture evolved HCF_3, thus indicating a further hydrolysis step [cf. Eq. (2)]. Finally, the remaining volatile $(CF_3)_2POH$ can be separated from the less volatile $CF_3P(O)(H)OH$ but the yields are low.

The cleavage of the P–N bond of amino phosphanes can also be performed by treatment with sulfonic acids.[12] In the first step, on reaction of $(CF_3)_2PNEt_2$ with sulfonic acid derivatives, $RS(O)_2OH$ ($R = CF_3$, $C_6H_4CH_3$), an unstable mixed anhydride $(CF_3)_2P{-}O{-}S(O)_2R$ is formed which itself has not been observed to date. Only the products of its rearrangement, the symmetric anhydrides $(CF_3)_2P{-}O{-}P(CF_3)_2$ and $RS(O)_2{-}O{-}S(O)_2R$ have been observed. The anhydride $(CF_3)_2P{-}O{-}P(CF_3)_2$ reacts in the presence of sulfonic acids to form $(CF_3)_2POH$ and unstable $(CF_3)_2P{-}O{-}S(O)_2R$, which in turn forms $(CF_3)_2P{-}O{-}P(CF_3)_2$ and $RS(O)_2{-}O{-}S(O)_2R$ (Scheme 1). In summary, reaction of at least three equivalents of the nonvolatile *p*-toluene sulfonic acid, suspended in the less-volatile solvent 1,6-dibromohexane with $(CF_3)_2PNEt_2$, results in a quantitative yield of $(CF_3)_2POH$. Because $(CF_3)_2POH$ is the only volatile compound in the

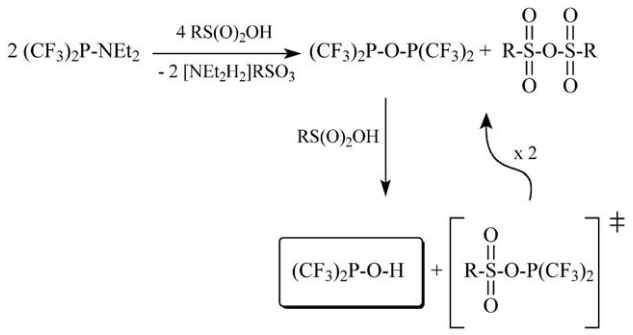

Scheme 1. One-step synthesis of $(CF_3)_2POH$. R = CF_3, $C_6H_4CH_3$.

complex reaction mixture, the product can be easily separated in a 90% yield by using fractional condensation.

A multinuclear NMR spectroscopic investigation of the obtained sample proved its purity. Surprisingly, the infrared spectrum of the gaseous sample exhibits two bands in the OH stretching region at $\tilde{\nu}$ = 3672 and 3598 cm^{-1} rather than one at 3620 cm^{-1} as was described by Burg and coworkers.[6,8] This discrepancy was already mentioned by Dobbie and Straughan in 1971, who assumed that two rotational isomers were responsible for the two different OH stretching modes.[13] Stimulated by this assumption, the potential energy[14] was calculated along the CPOH dihedral angle. For a complete rotation of the OH group, the energy scan (Figure 1) exhibits two minima. In the more-stable rotational isomer, the OH group is oriented *cis* relative to the C-P-C bisector whereas it is oriented *trans* in the less-stable rotational isomer (Figure 1). At the B3PW91/6-311G(3d,p) level of theory, the optimized rotational isomers, both with C_s symmetry, exhibit a zero-point-corrected energy difference of 5.9 kJ mol^{-1}. The activation barrier for the interconversion calculated by using the synchronous transit-guided quasi-Newton (STQN) method[14] at the same theoretical level was found to be ΔE_{ZP} = 12.6 kJ mol^{-1} (Figure 2).

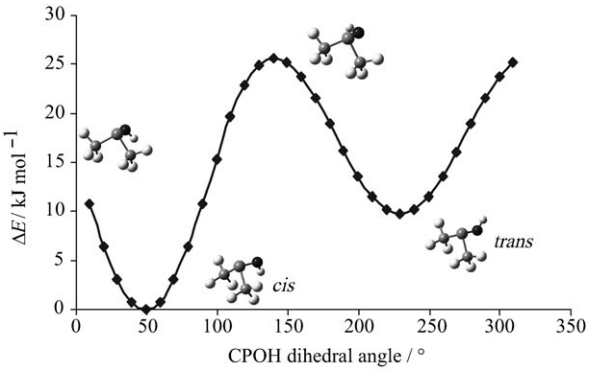

Figure 1. Potential energy of $(CF_3)_2POH$[14] along the CPOH dihedral angle.

The difference between the two calculated OH valence mode wavenumbers ($\tilde{\nu}$ = 3871 (*trans*) and 3783 cm^{-1} (*cis*)) of 88 cm^{-1} is in good agreement with the experimental value of 74 cm^{-1}, which proves the coexistence of two rotational isomers at room temperature. Due to the fast rotation of the P–OH group, a variable-temperature NMR spectroscopic investigation of the neat product, as well as that of dilute solutions in different kinds of solvents, did not allow the observation of rotational isomers.

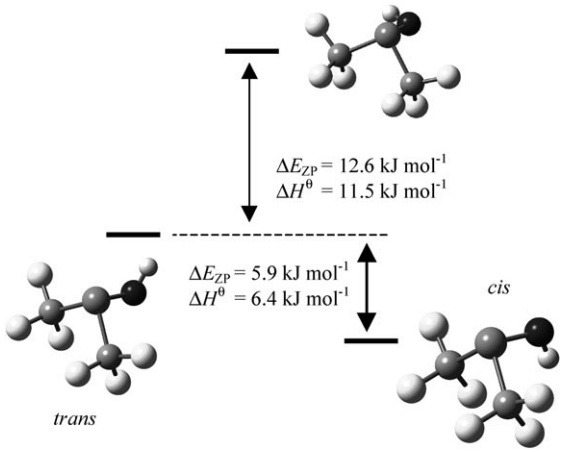

Figure 2. Rotational isomers of $(CF_3)_2POH$. The activation energy of the interconversion was calculated at the B3PW91/6-311G(3d,p) level using the STQN method.[14]

Vibrational spectra: The first IR study on gaseous $(CF_3)_2POH$ was performed by Griffiths and Burg more than 40 years ago and its feasible phosphane oxide structure $(CF_3)_2P(O)H$ was excluded.[8] One $\tilde{\nu}$(OH) stretching vibration was reported at 3620 cm^{-1} and, based on the wavenumber shifts upon deuteration, the bands at 1054 and 854 cm^{-1} were assigned as POH bending and P–OH stretching modes, respectively. Furthermore, the characteristic vibrations of the $(CF_3)_2P$ group were partly analyzed. Later, Dobbie and Straughan attributed a doublet splitting of the E–H stretching and PEH bending modes in $(CF_3)_2PEH$ (E = O, S) to rotational isomerism.[13] A temperature effect on the $\tilde{\nu}$(OH) bands in the IR spectrum of gaseous $(CF_3)_2POH$ was observed and an approximate value of 1 kcal mol^{-1} for the enthalpy difference between the conformers was estimated.

In the following, 1) the complete experimental vibrational spectra of both rotamers, 2) their predicted vibrational spectra obtained by quantum chemical calculations, and 3) an attempt at photoinduced isomerization of matrix-isolated $(CF_3)_2POH$ will be presented.

The gas-phase IR and solid-phase Raman spectra of $(CF_3)_2POH$ are depicted in Figure 3. All vibrational data observed in the gas phase, in a neon matrix, and for a liquid and solid Raman sample are listed in Table 1. The experimental wavenumbers are compared with predicted values from quantum chemical calculations and a tentative assignment of modes is given. By assuming C_s symmetry for the rotamers of $(CF_3)_2POH$, the 27 fundamentals for each species are represented as: Γ_{vib} = 15a′+12a″, in which the a′

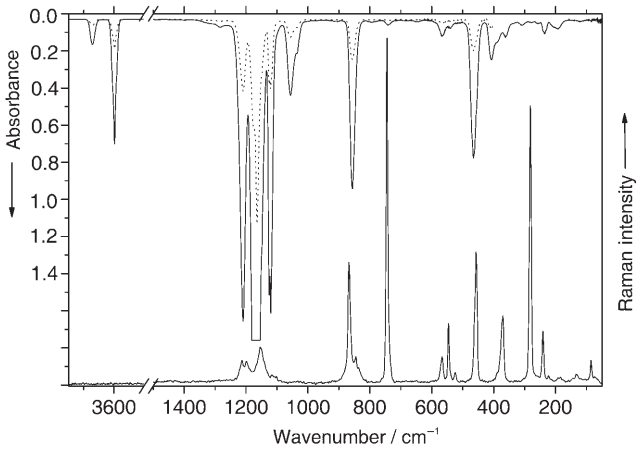

Figure 3. IR spectra of gaseous $(CF_3)_2POH$ (----- = 1.0 mbar, —— = 4.4 mbar in a 200 mm path length gas cell at room temperature) and Raman spectrum of solid $(CF_3)_2POH$ at −196 °C.

in-plane and a″ out-of-plane modes are all IR and Raman active. They can be divided into ten stretching, three torsional, and 14 bending modes. The two $\tilde{\nu}$(OH) bands at 3672 and 3598 cm^{-1} are due to the two rotamers. Because the weaker band at 3672 cm^{-1} increases with increasing temperature at the expense of the band at 3598 cm^{-1}, the weaker band must belong to the less-stable species. Assignment to *cis* or *trans* is in principle possible by analyzing the gas band contours. However, all gas band contours were faded and the less-stable species was found to be the *trans* rotamer by using quantum chemical calculations.

Numerous equilibrium mixtures of rotamers have been studied by using a trapped thermal effusive molecular beam as an inert gas matrix.[15] If the barrier of rotation in the molecule is greater than 5 kJ mol^{-1}, the conformational equilibrium is retained in the matrix. The calculated barrier for the isomerization of *trans*-$(CF_3)_2POH \rightarrow$*cis*-$(CF_3)_2POH$ amounts to about 15 kJ mol^{-1}, independent of the level of theory. Therefore, both rotamers should be seen in the IR matrix spectra. However, to our surprise, quenching of different equilibrium mixtures from the gas phase in Ar or Ne matrices at 12 or 6 K, respectively, yielded matrix-isolated *cis*-$(CF_3)_2POH$ exclusively in each case.

Table 1. Experimental and calculated fundamental wavenumbers ($\tilde{\nu}$ in cm^{-1}) and band intensities (I) of *cis*- and *trans*-$(CF_3)_2POH$.

IR gas (I)[a] *cis/trans*	Ne matrix (I)[b] *cis*	Raman[c] *cis*	Calculated[d] *trans*	*cis*		Assignment[e]/Approximate description of mode	
3672 (2.8)			3873(46)			*trans*	$\tilde{\nu}$(OH)
3598 (14)	3592.7 (22)			3784(27)	a′	$\tilde{\nu}_1$	$\tilde{\nu}$(OH)
1211 (35)	1213.0 (81)	1213 w	1223(79)	1210(100)	a′	$\tilde{\nu}_2$	$\tilde{\nu}_s(CF_3)$
1175 sh (54)	1175.7 (72)	1199 w	1179(100)	1174(95)	a′	$\tilde{\nu}_3$	$\tilde{\nu}_{as}(CF_3)$
1165 (100)	1163.0 (100)	1154 m	1170(36)	1162(57)	a′	$\tilde{\nu}_4$	$\tilde{\nu}_{as}(CF_3)$
			1154(23)	1156(80)	a″	$\tilde{\nu}_{16}$	$\tilde{\nu}_s(CF_3)$
1149 sh (27)	1146.0 (22)		1138(40)	1143(56)	a″	$\tilde{\nu}_{17}$	$\tilde{\nu}_{as}(CF_3)$
1120 (34)	1118.1 (50)		1117(71)	1114(37)	a″	$\tilde{\nu}_{18}$	$\tilde{\nu}_{as}(CF_3)$
1056 (9)	1057.6 (24)			1083(38)	a′	$\tilde{\nu}_5$	δ(POH)
1034 sh (4)			1083(58)			*trans*	δ(POH)
856 (20)	857.2 (36)	868 s,p		848(37)	a′	$\tilde{\nu}_6$	$\tilde{\nu}$(PO)
845 sh		845 w	835(28)			*trans*	$\tilde{\nu}$(PO)
741 (0.6)	741.6 (1)		750(0.5)	744(0.7)	a″	$\tilde{\nu}_{19}$	$\delta_s(CF_3)$
		745 vs,p	745(0.3)	740(0.8)	a′	$\tilde{\nu}_7$	$\delta_s(CF_3)$
566 (1.8)	567.2 (4)	566 m	563(4.1)	564(5.2)	a′	$\tilde{\nu}_8$	$\delta_{as}(CF_3)$
		546 m	544(0.2)	542(<0.1)	a′	$\tilde{\nu}_9$	$\delta_{as}(CF_3)$
539 (0.9)	541.4 (3)		542(0.4)	540(4.0)	a″	$\tilde{\nu}_{20}$	$\tilde{\nu}_{as}$(CPC)
		524 w	520(0.2)	519(0.9)	a″	$\tilde{\nu}_{21}$	$\delta_{as}(CF_3)$
465 (15)	470.4 (39)			482(48)	a″	$\tilde{\nu}_{22}$	τ(POH)
453 sh			461(6.8)			*trans*	τ(POH)
	456.5 (7)	457 s,p	450(5.9)	452(8.3)	a′	$\tilde{\nu}_{10}$	$\delta_{as}(CF_3)$
408 (4.5)	413.9 (15)			422(8.3)	a″	$\tilde{\nu}_{23}$	ω(POH)
387 sh (2)			360(0.3)			*trans*	ω(POH)
361 (2)		370 m,p	331(15)	359(3.0)	a′	$\tilde{\nu}_{11}$	$\rho(CF_3)$
307 (0.5)		281 vs,p	276(0.1)	277(0.1)	a′	$\tilde{\nu}_{12}$	$\tilde{\nu}_s$(CPC)
		241 m	257(2.9)	274(0.1)	a″	$\tilde{\nu}_{24}$	$\rho(CF_3)$
236 (1)			214(0.2)	229(3.1)	a″	$\tilde{\nu}_{25}$	$\rho(CF_3)$
193 (1)		184 vw	182(<0.1)	187(3.6)	a′	$\tilde{\nu}_{13}$	$\rho(CF_3)$
			163(0.2)	160(0.4)	a″	$\tilde{\nu}_{26}$	ρ(CPO)
		134 vw	117(0.3)	123(0.4)	a′	$\tilde{\nu}_{14}$	δ(CPC)
		85 w	70(0.2)	77(<0.1)	a′	$\tilde{\nu}_{15}$	$\tau(CF_3)$
			17(<0.1)	15(0.1)	a″	$\tilde{\nu}_{27}$	$\tau(CF_3)$

[a] Position and relative absorbance at band center. [b] Position at the most intensive matrix site. Intensity integrated over all matrix sites belonging to the respective fundamental. [c] Solid at −196 °C; "p" denotes polarized band of a liquid sample. [d] B3PW91/6-311G(3d,p); *cis* 100 % = 277.5 km mol^{-}; *trans* 100 % = 338.0 km mol^{-1}.[14] [e] Assignment for *cis* conformer. Types of vibration: $\tilde{\nu}$ = stretch, δ = bending, τ = torsion, ω = out-of-plane deformation, ρ = rocking.

Although $(CF_3)_2POH$ is a strong UV absorber (see Figure 4), photolysis of the matrices led neither to any isomers nor to decomposition products.

On closer inspection of the IR spectra of the gaseous sample at different temperatures, several band shoulders of variable intensity could be recognized at $\tilde{\nu}$ = 1034, 845, 453, and 387 cm^{-1}; these are assigned to the POH motions of the *trans* rotamer. For the *cis* rotamer, 25 fundamentals have been observed with $\tilde{\nu}_4/\tilde{\nu}_{16}$ and $\tilde{\nu}_{19}/\tilde{\nu}_7$ found to be accidentally degenerated. The assignment of all fundamentals is based on comparison with the calculated band position, intensity, and symmetry class; characteristic vibrations; as well as the polarization of some Raman bands of a liquid sample. The bands in the range $\tilde{\nu}$ = 600–100 cm^{-1} are more or less coupled and the description of modes is in part arbitrary.

Determination of the equilibrium: The clearly separated OH stretching modes at $\tilde{\nu}$ = 3672 and 3598 cm^{-1} are suitable for

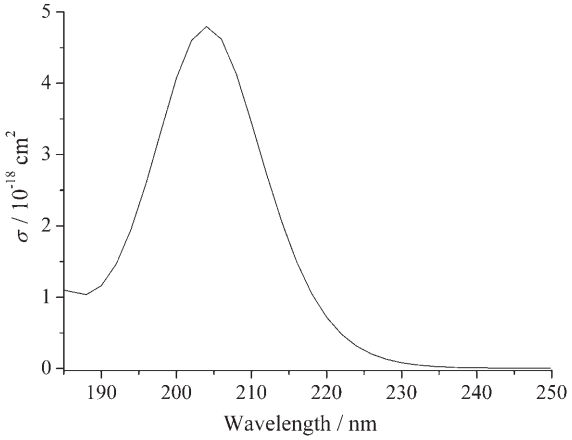

Figure 4. UV spectrum of gaseous $(CF_3)_2POH$ (λ_{max} = 206 nm). σ = absorption cross section.

the evaluation of the chemical thermodynamics of the interconversion process, shown in Equation (4):

$$trans\text{-}(CF_3)_2POH \rightleftharpoons cis\text{-}(CF_3)_2POH \quad (4)$$

In Figure 5, both gas-phase OH stretching bands at three different temperatures are depicted. It can be seen that with increasing temperature the absorption of the high frequency band increases at the expense of the low frequency band. Therefore, the peak at 3598 cm^{-1} must belong to the more stable *cis* rotamer, in accordance with quantum chemical calculations (see above).

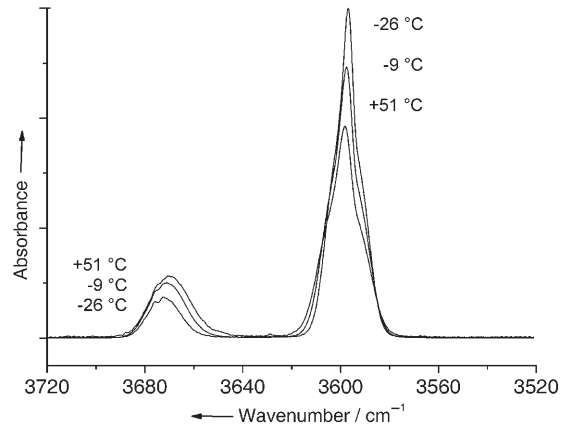

Figure 5. IR spectra of gaseous $(CF_3)_2POH$ in the $\tilde{\nu}$(OH) region at −26, −9, and +51 °C.

The differences in enthalpy and entropy of both rotamers were determined by the method of van't Hoff and Ulrich, shown in Equation (5):

$$\ln K_x = \ln\left(\frac{x_c}{x_t}\right) = -\frac{\Delta H^\circ}{RT} + \frac{\Delta S^\circ}{R} \quad (5)$$

in which *c* and *t* denote *cis* and *trans*, *x* the molar fraction, and *K* the equilibrium constant. In our experiment, *x* can be replaced by the integrated absorbance *A* and the extinction coefficient ε to give Equation (6):

$$\ln\left(\frac{x_c}{x_t}\right) = \ln\left(\frac{A_c}{A_t}\right) + \ln\left(\frac{\varepsilon_t}{\varepsilon_c}\right) \quad (6)$$

The *A* values can be measured directly from the spectra, whereas the ratio of the extinction coefficients ($\varepsilon_c/\varepsilon_t$) is available only from experiments at different temperatures. The measured data at seven different temperatures are gathered in Table 2. The total concentration of both rotamers of

Table 2. Input data for the determination of the equilibrium constants.

T [K]	*p* [mbar]	A[a] *cis*	*trans*	A_c/A_t	K_p	$\ln(K_p)$
351.1	4.44	7.7668	2.7072	2.87	3.20	1.164
326.2	3.85	8.0598	2.4706	3.26	3.64	1.292
299.9	4.13	9.8155	2.4641	3.98	4.44	1.491
273.7	4.02	1.8545	2.2140	5.12	5.72	1.743
264.1	3.40	9.6301	1.6933	5.69	6.35	1.849
253.8	3.45	9.4117	1.5257	6.17	6.89	1.930
246.9	3.44	10.6461	1.6213	6.57	7.33	1.993

[a] Integrated absorbances for $\tilde{\nu}$(OH); $\tilde{\nu}_{cis}$ = 3598 cm^{-1}, $\tilde{\nu}_{trans}$ = 3672 cm^{-1}.

$(CF_3)_2POH$ in the gas cell is proportional to the pressure/temperature ratio (p/T) and the individual concentrations are proportional to the absorbance/extinction coefficient ratio (A/ε). Hence, at any temperature and pressure, Equation (7) is valid:

$$\frac{p}{T} \approx \frac{A_c}{\varepsilon_c} + \frac{A_t}{\varepsilon_t} \quad (7)$$

which can be rearranged to give Equation (8):

$$\frac{A_t T}{p} \approx \varepsilon_t - \frac{(\varepsilon_t/\varepsilon_c)A_c T}{p} \quad (8)$$

The normalized integrated absorbances $(AT)/p$ for the OH stretching bands of both rotamers form a straight line, as shown in Figure 6, for which the slope $\varepsilon_t/\varepsilon_c$ = 1.16. The two points obtained at the highest and lowest temperature did not fit the straight line well and have therefore not been used for the regression. At the highest temperature some decomposition of the sample occurred and at the lowest temperature a little sample was deposited on the silicon windows, which disturbed the total concentration of gaseous $(CF_3)_2POH$ in the IR beam. The ratio $\varepsilon_t/\varepsilon_c$ obtained from quantum chemical calculations (1.70, cf. Table 1) is noticeably larger. The reason for the deviation remains unclear. With the experimental $\varepsilon_t/\varepsilon_c$ ratio on hand, the absorbance ratio can be converted into the molar ratio (K_p, Table 2) and the data are plotted in Figure 7. The regression yields $\Delta H^\circ = -5.92 \pm 0.14$ kJ mol^{-1} and $\Delta S^\circ = -7.28$ J mol^{-1} K^{-1}, aver-

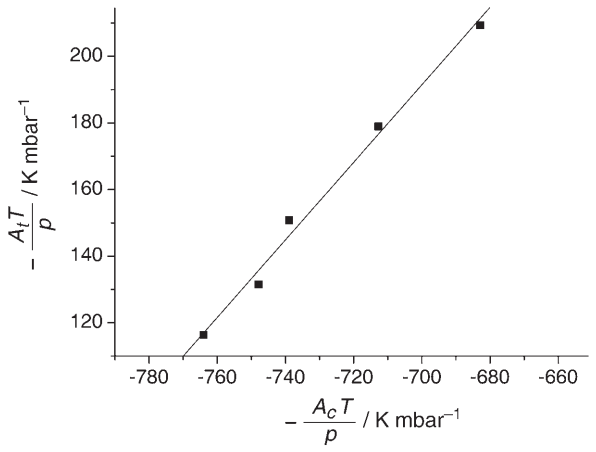

Figure 6. Plot of the integrated absorbances of the $\tilde{\nu}$(OH) IR bands of *cis* (A_c) and *trans* (A_t) $(CF_3)_2POH$, normalized to the total concentration (T/p). The slope represents the relative IR intensities of the $\tilde{\nu}$(OH) bands.

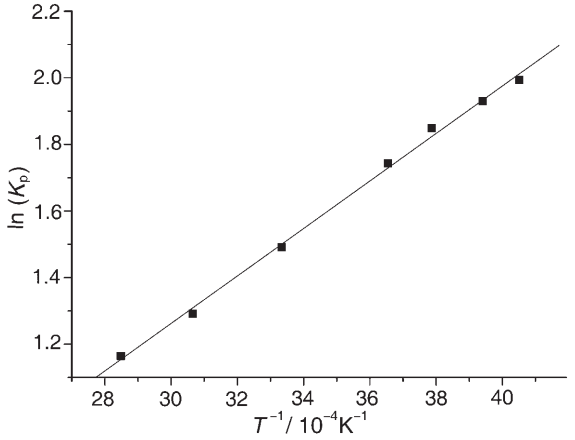

Figure 7. Van't Hoff plot of the gas-phase equilibrium of *cis*/*trans*-$(CF_3)_2POH$.

aged over the temperature range used. The uncertainty in ΔH° is mainly due to errors in the determination of the temperature and of K_p, whereas that for ΔS° is due to errors in the proportionality factor and in ΔH°.

The reaction enthalpy, ΔH°, for the conversion of *trans*-$(CF_3)_2POH$ to *cis*-$(CF_3)_2POH$ is in excellent agreement with the predicted (B3PW91/6-311G(3d,p)) value of $-6.40\,kJ\,mol^{-1}$. However, the calculated reaction entropy, ΔS°, of $-3.10\,J\,mol^{-1}\,K^{-1}$ is lower than the experimental value. The calculated entropy difference depends strongly on the low frequency CF_3 torsional vibrations in the two conformers, with the torsions of the *cis* species being higher in frequency on account of its intramolecular hydrogen bridge. The torsional frequencies are predicted to be in the range between 10 and 20 cm^{-1}, and thus make contributions to the entropy of about $30\,J\,mol^{-1}\,K^{-1}$. Because the calculation of such low vibrational frequencies is not very reliable, the calculated entropy difference is not reliable either.

At room temperature (22 °C) the composition in the equilibrium amounts to 82% *cis* and 18% *trans*. These values were used in the electron-diffraction study.

Structure analysis—electron diffraction: Averaged molecular intensities in the s ranges of 0.02–0.18 and 0.08–0.35 pm^{-1} in steps (Δs) of 0.002 pm^{-1} ($s = (4\pi/\lambda)\sin\theta/2$, λ = electron wavelength, θ = scattering angle) are shown in Figure 8. The radial-distribution function (RDF) was de-

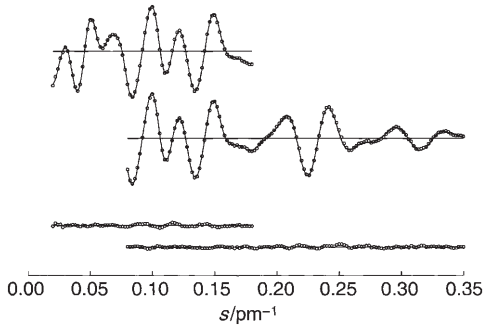

Figure 8. Experimental and calculated molecular intensities for long (above) and short (below) nozzle-to-plate distances and residuals.

rived by Fourier transformation of these intensities, by applying an artificial damping function $\exp(-\gamma s^2)$ with γ = 19 pm[14] (Figure 9). The experimental RDF is not sensitive towards the orientation of the O–H bond. The geometric parameters of the prevailing *cis* form were refined by least-squares fitting of the molecular intensities. The overall symmetry was constrained to C_s symmetry. Local C_{3v} symmetry with a possible tilt angle between the C_3 axis and the P–C bond direction was assumed for the CF_3 groups. The O–H bond length and P-O-H angle were not refined. Vibrational amplitudes were collected in groups according to their cal-

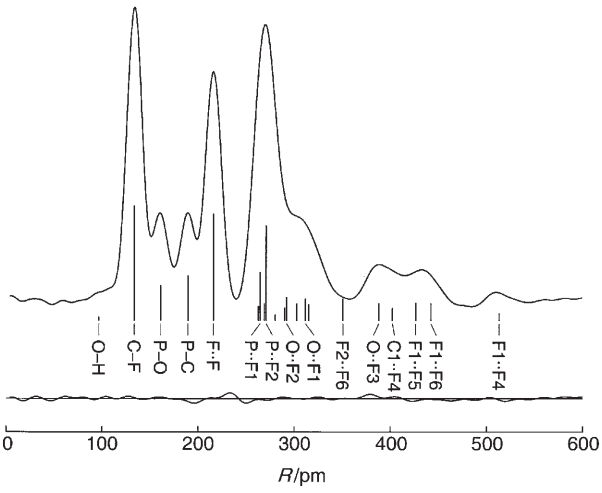

Figure 9. Experimental radial-distribution function and difference curve. The position of important interatomic distances are indicated by vertical bars.

culated values. Geometric parameters of the *trans* conformer were tied to those of the *cis* form by using the calculated differences. The ratio of both conformers was set to the value derived from the vibrational data. With these assumptions, eight geometric parameters and ten vibrational amplitudes ($l1$ to $l10$) were refined simultaneously. The following correlation coefficients had absolute values larger than 0.7: CF/FCF = 0.71, OPC/$l8$ = 0.75, tilt(CF_3)/$l5$ = −0.93, and τ(CF_3)/$l9$ = 0.82. The results of the least-squares analysis are given in Table 3 (geometric parameters) and Table 4 (vibrational amplitudes) together with the calculated values, and a molecular model is presented in Figure 10.

Table 3. Experimental and calculated geometric parameters for the *cis* conformer.

	GED[a]	MP2/6-311G(3d,p)	B3LYP/6-311G(3d,p)
P–O	166.1(4)	163.2	162.7
P–C	189.5(3)	188.5	189.9
C–F	133.9(1)	134.5	134.1
O–H	97.0[d]	97.0	96.7
C-P-C	95.4(10)	95.7	96.9
O-P-C	99.8(15)	98.9	99.3
F-C-F	107.6(3)	107.6	107.7
P-O-H	112.2[d]	113.1	113.8
tilt(CF_3)[b]	2.9(12)	2.1	3.7
τ(CF_3)[c]	−5.6(39)	−2.9	−3.9

[a] r_a values in pm and °. Error limits are 3σ values and refer to the last digit. [b] Tilt angle between C_3 axis and P–C bond direction in CPC plane and away from the opposite P–C bond. [c] Torsional angle of CF_3 group. τ(CF_3) = 0° for the exact staggered orientation. A negative value implies shortening of the F2···F5 distance (see Figure 10 for atom numbering). [d] Not refined.

Table 4. Interatomic distances and experimental and calculated vibrational amplitudes (without distances involving hydrogen).[a]

	Distance	Ampl. (GED)		Ampl. (MP2)[a]
C–F	134	4.4(2)	$l1$	4.5
P–C	161	4.4(2)	$l1$	4.4
P–C	190	4.7(4)	$l2$	5.2
F···F	216	5.7(2)	$l3$	5.7
F2···F5	263	43.2 (254)	$l4$	40.1
P···F	264–271	8.1(6)	$l5$	8.2
C···O	269	8.8[b]		8.8
C1···C2	280	8.1(6)	$l5$	7.8
F3···F6	290	43.2(254)	$l4$	41.0
O···F2	292	15.0(16)	$l6$	40.8
C1···F5	303	15.0(16)	$l6$	42.6
O···F1	312	15.0(16)	$l6$	45.2
C1···F6	315	15.0(16)	l6	43.6
F2···F6	351	43.2(254)	$l4$	98.8
O···F3	388	10.5(18)	$l7$	15.7
C1···F4	402	17.8(114)	$l8$	11.9
F1···F5	426	13.9(55)	$l9$	22.5
F1···F6	442	13.9(55)	$l9$	24.3
F1···F4	513	9.3(30)	$l10$	10.0

[a] Values in pm, error limits are 3σ values. For atom numbering see Figure 10. Vibrational amplitudes were derived from a calculated (MP2/6-31G(d,p)) force field,[14] using the method of Sipachev.[16] [b] Not refined.

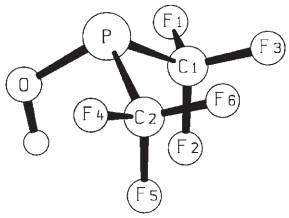

Figure 10. Molecular model with atom numbering.

Experimental Section

Synthesis of bis(trifluoromethyl)phosphinous acid: *p*-Toluenesulfonic acid monohydrate (20 g, 105 mmol), dried at room temperature for 12 h at 5×10^{-4} mbar, was suspended in 1,6-dibromohexane (200 mL). After degassing the resulting brown suspension for one hour under vacuum, $(CF_3)_2PNEt_2$[10] (5.5 g, 23 mmol) was added using a syringe. After stirring the suspension for 12 h at room temperature, the brown color disappeared. The volatile compounds were removed under dynamic vacuum conditions by using three traps at −30, −78, and −196 °C to separate minor amounts of the solvent, $(CF_3)_2POH$ and HCF_3. The −78 °C trap contained 3.7 g (20 mmol, 88 %) of a colorless liquid identified as $(CF_3)_2POH$. The product can be stored for several months in sealed glass ampoules at room temperature and exhibits no sign of decomposition. NMR (neat, RT): ^{1}H NMR: δ = 4.4 ppm (s); ^{13}C NMR: δ = 125.7 ppm (q, d, q) (^1J(P,C) = 30.0 Hz, ^1J(C,F) = 320.7 Hz, ^3J(C,F) = 7.5 Hz); ^{19}F NMR: δ = −69.3 ppm (d); ^{31}P NMR: δ = 77.9 ppm (sept) (^2J(P,F) = 83.1 Hz).

Vibrational spectra: Raman spectra of a liquid and a solid sample were recorded on an FT-Raman spectrometer (Equinox 55/FRA 106 s^{-1}, Bruker) using a 500 mW Nd:YAG laser (λ = 1064 nm), a Si/CaF_2 beam splitter, and a liquid-nitrogen-cooled NIR detector D418-T. The liquid sample was placed in a sealed 4 mm glass capillary and the solid sample was condensed as a spot on a nickel finger at −196 °C under high vacuum. For each spectrum, 128 scans were averaged at an apodized resolution of 2 cm^{-1}.

Infrared spectra were measured with an IFS 66v FTIR spectrometer (Bruker) employing resolutions of 1 or 2 cm^{-1} using a KBr/Ge or a 6 μm-Mylar/Ge beamsplitter and DTGS detectors. For each spectrum, 64 scans were averaged.

Infrared spectra of the gaseous sample in the temperature range −26 to 78 °C were obtained by using a temperature-controlled gas cell with an optical path length of 20 cm. The double-walled glass cell equipped with silicon windows (0.5 mm thick) and a Pt-100 temperature sensor was placed inside the evacuated (< 2 mbar) sample chamber of the spectrometer. The cell was filled with $(CF_3)_2POH$ vapor and evacuated from outside the spectrometer. Pressure control was accomplished by the use of a Baratron pressure transducer (type 122A, 10 mbar, accuracy 10^{-3} mbar). Temperature control was achieved to better than 1 °C by a flow of cooled or heated air. In order to prevent systematic errors in the pressure readings due to decomposition of $(CF_3)_2POH$ or impurities from the cell, for each experiment at every temperature, a new sample was taken from the $(CF_3)_2POH$ reservoir.

Infrared spectra of matrix-isolated samples of equilibrium mixtures *cis*/*trans*-$(CF_3)_2POH$/Ar (or Ne) at different temperatures were obtained by trapping the molecular beam at 12 or 6 K, respectively. Details of the matrix-isolation apparatus are given elsewhere.[17,18]

Electron diffraction: Electron diffraction intensities were recorded with a Gasdiffraktograph KD-G2[19] at 25 and 50 cm nozzle-to-plate distances and with an accelerating voltage of about 60 kV. The sample was cooled to −18 °C and the inlet system and nozzle were at room temperature. The photographic plates were analyzed with an Agfa Duoscan HiD scanner and total-scattering-intensity curves were obtained from the TIFF-file using the program SCAN3.[20]

Acknowledgements

Dr. K. Glinka is acknowledged for helpful discussions. The Deutsche Forschungsgemeinschaft and the Fonds der Chemischen Industrie are acknowledged for financial support.

[1] D. E. C. Corbridge, *Phosphorus: An Outline of its Chemistry, Biochemistry and Uses*, Elsevier, Amsterdam, **1995**, 5th ed., p. 336.
[2] J. Chatt, B. T. Heaton, *J. Chem. Soc. A* **1968**, 2745–2757.
[3] N. V. Dubrovina, A. Börner, *Angew. Chem.* **2004**, *116*, 6007–6010; *Angew. Chem. Int. Ed.* **2004**, *43*, 5883–5886, and references therein.
[4] B. Hoge, C. Thösen, T. Herrmann, P. Panne, I. Pantenburg, *J. Fluorine Chem.* **2004**, *125*, 831–851.
[5] B. Hoge, W. Wiebe, S. Hettl, S. Neufeind, C. Thösen, *J. Organomet. Chem.* **2005**, *690*, 2382–2387.
[6] J. E. Griffiths, A. B. Burg, *J. Am. Chem. Soc.* **1960**, *82*, 1507–1508.
[7] J.-L. Virlichie, P. Dagnac, *Rev. Chim. Miner.* **1977**, *14*, 355–358.
[8] J. E. Griffiths, A. B. Burg, *J. Am. Chem. Soc.* **1962**, *84*, 3442–3450.
[9] W. Ruppert, I. Ruppert, *Tetrahedron Lett.* **1983**, *24*, 5509–5512.
[10] A. Kolomeitsev, M. Görg, U. Dieckbreder, E. Lork, G.-V. Röschenthaler, *Phosphorus Sulfur Silicon Relat. Elem.* **1996**, *109–110*, 597–600.
[11] B. Hoge, C. Thösen, *Inorg. Chem.* **2001**, *40*, 3113–3116.
[12] W. Dabkowski, J. Michallski, Skrzypczński, *J. Chem. Soc. Chem. Commun.* **1982**, 1260–1261.
[13] R. C. Dobbie, B. P. Straughan, *Spectrochim. Acta Sect. A* **1971**, *27*, 255–260.
[14] Gaussian 03, Revision B.04, M. J. Frisch, G. W. Trucks, H. B. Schlegel, G. E. Scuseria, M. A. Robb, J. R. Cheeseman, J. A. Montgomery, Jr., T. Vreven, K. N. Kudin, J. C. Burant, J. M. Millam, S. S. Iyengar, J. Tomasi, V. Barone, B. Mennucci, M. Cossi, G. Scalmani, N. Rega, G. A. Petersson, H. Nakatsuji, M. Hada, M. Ehara, K. Toyota, R. Fukuda, J. Hasegawa, M. Ishida, T. Nakajima, Y. Honda, O. Kitao, H. Nakai, M. Klene, X. Li, J. E. Knox, H. P. Hratchian, J. B. Cross, V. Bakken, C. Adamo, J. Jaramillo, R. Gomperts, R. E. Stratmann, O. Yazyev, A. J. Austin, R. Cammi, C. Pomelli, J. W. Ochterski, P. Y. Ayala, K. Morokuma, G. A. Voth, P. Salvador, J. J. Dannenberg, V. G. Zakrzewski, S. Dapprich, A. D. Daniels, M. C. Strain, O. Farkas, D. K. Malick, A. D. Rabuck, K. Raghavachari, J. B. Foresman, J. V. Ortiz, Q. Cui, A. G. Baboul, S. Clifford, J. Cioslowski, B. B. Stefanov, G. Liu, A. Liashenko, P. Piskorz, I. Komaromi, R. L. Martin, D. J. Fox, T. Keith, M. A. Al-Laham, C. Y. Peng, A. Nanayakkara, M. Challacombe, P. M. W. Gill, B. Johnson, W. Chen, M. W. Wong, C. Gonzalez, J. A. Pople, Gaussian, Inc., Wallingford CT, **2004**.
[15] A. J. Barnes in *Matrix Isolation Spectroscopy, NATO ASI, Series C, Vol. 76* (Eds.: A. J. Barnes, W. J. Orville-Thomas, A. Müller, R. Guafrés), Reidel, Dordrecht, Holland, **1981**.
[16] a) V. A. Sipachev, *THEOCHEM.* **1985**, *121*, 143–151; b) V. A. Sipachev, *Adv. Mol. Struct. Res.* **1999**, *5*, 263–311; c) V. A. Sipachev, *NATO Sci. Ser. II* **2002**, *68*, 73–90.
[17] M. Bodenbinder, S. E. Ulic, H. Willner, *J. Phys. Chem.* **1994**, *98*, 6441–6444.
[18] H. Schnöckel, H. Willner in *Infrared and Raman Spectroscopy, Methods and Applications* (Ed.: B. Schrader), VCH, Weinheim, **1994**, p. 294.
[19] H. Oberhammer, *Molecular Structure by Diffraction Methods, Vol. 4*, The Chemical Society, London, **1976**, 24–44.
[20] E. G. Atavin, L. V. Vilkov, *Instrum. Exp. Tech. (in Russian)* **2002**, *45*, 27–32.

Received: August 30, 2005
Published online: February 21, 2006

